Defect Auger exciton dissociation and impact ionization in conjugated polymers

Chia-Hsin Chen* and Hsin-Fei Meng†
Institute of Physics, National Chiao Tung University, Hsinchu 300, Taiwan, Republic of China
(Received 6 November 2000; revised manuscript received 7 March 2001; published 6 September 2001)

We study theoretically the exciton dissociation and carrier generation in conjugated polymers via defect Auger process, in which the electron (hole) of the exciton drops into the deep defect level while the energy is released to the hole (electron) through Coulomb scattering. Contrary to the usual Auger process among free carriers at high densities, defect Auger process for excitons takes place independent of the exciton density, and is identified as the dominant mechanism of photocarrier generation for excitation below the band gap. The dissociation probability for each passage through the defect is found to be close to one for excitons with thermal velocity, consistent with the picture that exciton decay in oxidized polymers is controlled by diffusion on a chain with quenching centers . We also study the reverse process, i.e., defect impact ionization, in which excitons or free electron hole pairs are created via the impact of hot holes (electrons) on electrons (holes) in the defect level. Excitons are found to be produced predominantly for driving electric field in a window around 10^5 V/cm along the chain. Light emission under unipolar carrier injection is predicted.

DOI: 10.1103/PhysRevB.64.125202 PACS number(s): 72.80.Le, 73.50.Pz

I. INTRODUCTION

The past ten years has witnessed tremendous progress in both the science and technologies of light-emitting devices based on conjugated polymers.[1] Yet many fundamental questions regarding the two single important properties, electroluminescence (EL) and photoconductivity (PC), remain unanswered. The defects in the polymer chain, either structural or chemical, are believed to play an important role in both EL and PC. The deep electronic levels associated with the defects provide a convenient way to facilitate the dissociation of the exciton, and limit the luminescence quantum yield in EL. On the other hand, excitons must be dissociated in order to produce charge carriers for PC for excitation below the continuum threshold.[2] Even though the enhancement of PC and reduction of EL by oxidation, presumably due to exciton dissociation at the carbonyl defects, has been reported experimentally,[3] the microscopic mechanism which controls the dissociation rate is not well understood.

An exciton dissociation mechanism, the defect Auger process, is studied in this work. In this process the electron (hole) in the exciton drops into the empty (occupied) deep level while the hole (electron) is released by Coulomb scattering and becomes a free charge carrier with high kinetic energy as required by energy conservation. The corresponding Coulomb matrix element is shown in Figs. 1(a)and 1(b). The defect Auger process for exciton is in sharp contrast with the usual free carrier Auger process, which occurs only at high carrier concentrations because the relaxation energy of one free carrier is carried away by the kinetic energy of another nearby free carrier. Therefore the Auger rate usually depends strongly on the free carrier density and consequently the excitation level. On the other hand, in conjugated polymers the electron-hole pair remains bound to form exciton even at room temperature. So when one of the carrier relaxes there is always another oppositely charged carrier nearby to carry away the relaxation energy. In other words, each exciton can act alone and the dissociation rate is independent of the exciton density. This unique mechanism is expected to be quite efficient because the effective carrier distance, the exciton Bohr radius, is very small compared with the mean distance among the excited free carriers. If we use the material parameters suitable for poly (*para*-phenylene vinylene)

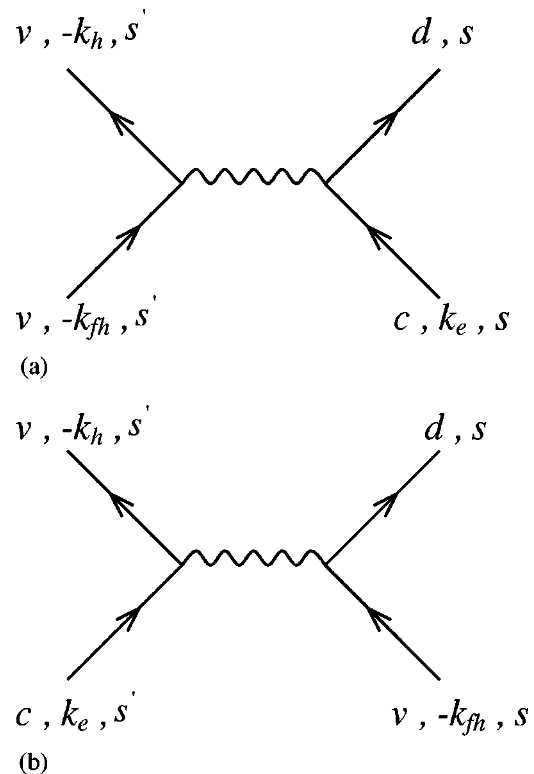

FIG. 1. (a) Diagram for the direct Coulomb scattering term in which one conduction electron (c,k_e,s) is captured by defect (d), while one free valence electron $(v,-k_{\rm fh},s')$ is scattered to $(v,-k_h,s')$. k is the wave number, and s is the spin index. (b) Diagram for the exchange Coulomb scattering term in which one valence electron $(v,-k_{\rm fh},s)$ is captured by defect, while one conduction electron (c,k_e,s') is scattered to the valence band state $(v,-k_h,s')$.

 ©2001 The American Physical Society

(PPV) and assume, as in the case of inorganic semiconductor, that each exciton samples the average defect density by interacting with many defects within its lifetime (the volume dissociation regime), our calculation shows that the rate is of the order of 10^{16} s^{-1} times the number of defect per repeat unit, which is expected to be no less than 10^{-3}. Such a high rate is three orders of magnitude faster than the more common multiphonon emission process.[2] Moreover, it can happen even at zero temperature because no energy barrier is present, consistent with the sweep-out regime experiment.[4] The defect Auger process is therefore identified as the primary microscopic origin for the photocarrier generation and luminescence quenching in conjugated polymers. The calculated dissociation rate can not, however, be used naively to obtain the PL and PC yield quantitatively. For example, the dissociation rate is of the order of 10^{13} s^{-1} with defect density equal to one per 400 repeat unit. The corresponding nonradiative lifetime would be around 0.1 ps. This value is four order of magnitude shorter than the radiative lifetime of the excitons, and implies that the light emission would be completely quenched if the decay were in the volume dissociation regime. This is, however, inconsistent with the experiment that the PL yield is reduced to only half at such defect density.[5] The reason is that the exciton dissociation process is not in the volume capture regime, in which each exciton encounters many defects before decay and a uniform exciton density is maintained throughout the system volume. Instead, the decay is in the diffusion regime,[5] in which the excitons do not have the chance to sample the average defect density but are immediately quenched by the first defect they hit along the path of their diffusive motion in the chain. In this case, the deep levels act as a black hole and no exciton can pass through it. Unlike the volume dissociation regime, in the diffusion regime the steady state exciton density is not uniform along the chain but vanishes at the defect positions. The decay dynamics of the total number of excitons, controlled not only by the the transition matrix element but also the diffusion coefficient of the excitons, is therefore not a simple exponential. We confirm this picture by calculating the dissociation probability of one single passage of the exciton through the defect with arbitrary incident velocity. The result is indeed close to one for excitons with thermal velocity.

In addition to the Auger process, we also study the rate of its reverse process, the defect impact ionization, by slightly modifying the calculations. Interestingly, in defect impact ionization the incident hot hole can kick out the electron in the deep level and form a neutral exicton with itself when the incident kinetic energy reaches the threshold. The number of charge carriers is reduced from one to zero, in sharp contrast with the usual impact ionization for which the number of carriers multiplies and causes avalanche breakdown eventually. If the kinetic energy of the incident hot hole is increased further, it becomes possible to create a free electron-hole pair and the number of carriers multiplies as usual. In this circumstance the channel for carrier decrease (exicton production) and increase (free pair production) compete. Impact ionization coefficient to neutral exciton is found to be around 10^8/cm times the number of defect per repeat unit when holes are driven by the electric field around 10^5 V/cm. Exicton production by impact ionization opens the possibility of light emission under unipolar charge injection.

In Sec. II, the defect Auger dissociation rate for exciton as a function of the incident exciton momentum is calculated. The matrix element is derived in the Appendix. In Sec. III, the rate for defect impact ionization as a function of the incident hot hole momentum is calculated. Two possible final states, the exciton (Sec. III A) and the free electron-hole pair (Sec. III B), with different impact thresholds are considered. Averaged impact ionization coefficient for holes under high electric field is calculated in Sec. III C. We discuss and conclude in Secs. IV and V, respectively.

II. DEFECT AUGER DISSOCIATION OF EXCITON

We start with the total Hamiltonian $H=H_0+V$ for the $\pi-$electrons of a conjugated polymer chain with one deep level, where the one-particle part is

$$H_0=\sum_{\mu,k} E_\mu(k)a^\dagger_{\mu,k}a_{\mu,k}+E_d a^\dagger_d a_d, \tag{1}$$

and the two-body Coulomb interaction is

$$V=\frac{1}{2}\int d^3\mathbf{r}_1 d^3\mathbf{r}_2 \hat{\psi}^\dagger(\mathbf{r}_1)\hat{\psi}^\dagger(\mathbf{r}_2)\frac{e^2}{4\pi\epsilon\epsilon_0|\mathbf{r}_1-\mathbf{r}_2|}\hat{\psi}(\mathbf{r}_1)\hat{\psi}(\mathbf{r}_2). \tag{2}$$

The field operator $\hat{\psi}$ can be expanded as $\hat{\psi}(\mathbf{r}) \equiv\sum_{\mu,k}\psi_{\mu,k}(\mathbf{r})a_{\mu,k}+\psi_d(\mathbf{r})a_d$. k is the allowed wave number in the Brillouin zone, and $\mu=c,v$ is the band index for conduction and valence bands, respectively. $E_\mu(k)$ is the band disperson. E_d is the deep level energy. $\psi_{\mu,k}(\mathbf{r})$ is the Bloch wave function, and $\psi_d(\mathbf{r})$ is the deep level wave function. $a_{\mu,k}$, $a^\dagger_{\mu,k}$, and a_d, $a^\dagger_d$ are the corresponding annihilation and creation operators. After substituting the expansion of $\hat{\psi}(\mathbf{r})$ into V, the Coulomb interaction V can be divided into two parts : $V=V_f+V_d$, where V_f contains only the terms with Bloch state operators, while V_d contains the terms that involve at least one defect operators. It is well known that V_f is strong in conjugated polymers and causes the large exciton binding energy of the excitons. On the other hand, the residual Coulomb interaction V_d involving scattering of Bloch states into and out of the deep level is expected to be weak. Consequently we consider the free part of the Hamiltonian as H_0+V_f, and treat V_d as the perturbation which cause transitions between degenerate eigenstates of H_0+V_f.

A. Free carrier matrix element

Neglecting the free carrier Coulomb interaction V_f and therefore the exciton effect first. The defect Auger process is a two-body electron-hole Coulomb scattering $e(k_e)+h(k_h) \rightarrow e(d)+h(k_{\mathrm{fh}})$, in which one free electron (e) with wave number k_e drops into the deep defect level (d) while a hole (h) with wave number k_h is scattered to k_{fh} to compensate

the energy lost by the electron. ''fh'' denotes free hole. It can be expressed by the equivalent electron-electron scattering $e_c(k_e)+e_v(-k_{\rm fh})\rightarrow e(d)+e_v(-k_h)$, where c,v denote conduction and valence band, respectively. The transition matrix element of this process is $M_{e-h}=\langle d,-k_{\rm fh}|V_d|k_e,-k_h\rangle$, where $|k',k\rangle\equiv a^\dagger_{c,k'}a_{v,k}|g\rangle$ for the initial state, and $|d,k\rangle\equiv a^\dagger_d a_{v,k}|g\rangle$ for the final state. $|g\rangle$ is the ground state with filled valence band and empty conduction band. The spin indices are omitted first, and considered afterwards. After substituting the expansion of $\hat{\psi}$ into V_d in $M_{e\text{-}h}$, only two combinations, the direct term and the exchange term, survive. For a spin singlet initial electron-hole pair, the direct term is [Fig. 1(a)]

$$M_D(k_e,k_h,k_{\rm fh})=\frac{1}{2}\int \psi_d^*(\mathbf{r}_1)\psi^*_{v,-k_h}(\mathbf{r}_2)\frac{e^2}{4\pi\epsilon\epsilon_0|\mathbf{r}_1-\mathbf{r}_2|}\times\psi_{v,-k_{\rm fh}}(\mathbf{r}_2)\psi_{c,k_e}(\mathbf{r}_1)d^3\mathbf{r}_1d^3\mathbf{r}_2, \tag{3}$$

and the exchange term is [Fig. 1(b)]

$$M_E(k_e,k_h,k_{\rm fh})=\frac{1}{2}\int \psi_d^*(\mathbf{r}_1)\psi^*_{v,-k_h}(\mathbf{r}_2)\frac{e^2}{4\pi\epsilon\epsilon_0|\mathbf{r}_1-\mathbf{r}_2|}\times\psi_{c,k_e}(\mathbf{r}_2)\psi_{v,-k_{\rm fh}}(\mathbf{r}_1)d^3\mathbf{r}_1d^3\mathbf{r}_2. \tag{4}$$

The $\mathbf{r}_1$ and $\mathbf{r}_2$ integrals are performed in the Appendix. After some approximations, the final results are

$$M_D(K,k_h,k_{\rm fh})=\frac{\alpha_c}{\sqrt{N}}\frac{e^2}{4\pi\epsilon\epsilon_0 aN}e^{-i(k_{\rm fh}-K+\pi/a)R_d}m_D(k_{\rm fh},k_h), \tag{5}$$

$$m_D(k_{\rm fh},k_h)=\frac{4\pi\epsilon\epsilon_0 a}{2e^2}U-\ln\left[2\left|\sin\frac{(k_{\rm fh}-k_h)a}{2}\right|\right] \tag{6}$$

and

$$M_E(K,k_{\rm fh})=\frac{2\alpha_v}{\sqrt{N}}\frac{e^2}{4\pi\epsilon\epsilon_0 aN}e^{-i(k_{\rm fh}-K+\pi/a)R_d}m_E(K), \tag{7}$$

$$m_E(K)=\gamma\left\{\frac{4\pi\epsilon\epsilon_0 a}{2e^2}U-\ln\left[2\left|\sin\left(\frac{Ka}{2}\right)\right|\right]\right\}. \tag{8}$$

$K\equiv k_e+k_h$ is the total momentum of the electron-hole pair in the initial state divided by $\hbar$. R_d is the position of the defect. U is the on-site Coulomb repulsion energy for the direct term. For the exchange term, the matrix element is reduced by an overall factor γ, as defined in Eq. (A9). ϵ is the effective dielectric constant along the chain. a is the lattice constant. N is the total number of repeat unit of the chain. The expression for the overlaps $\alpha_{c,v}$ between the defect and Bloch states can be found in Eqs. (A5) and (A8) within the ''zero-radius potential'' approximation. π/a is the wave number at the direct band gap. For a triplet pair, the result of M_E is zero. We consider only the singlet pair below because it is more relevent for the PC and EL processes. Adding M_D and M_E together we get the matrix element $M_{e\text{-}h}$ for a electron-hole pair

$$M_{e\text{-}h}(K,k_h,k_{\rm fh})=M_D(K,k_h,k_{\rm fh})+M_E(K,k_{\rm fh})=\frac{2e^2}{4\pi\epsilon\epsilon_0 aN^{3/2}}e^{-i(k_{\rm fh}-K+\pi/a)R_d}\times\{\alpha_c m_D(k_{\rm fh},k_h)+2\alpha_v m_E(K)\}. \tag{9}$$

B. Exciton matrix element

Due to the Coulomb attraction V_f between the electron and the hole, the elementary excitation of the free part of the Hamiltonian H_0+V_f is no longer a free electron-hole pair but a superposition of them, i.e., the exciton state, labeled by $|\text{ex};K\rangle$. $K=k_e+k_h$ is the new exciton center of mass wave number. $|\text{ex};K\rangle$ is the initial state of the dissociation process, while the final state is still $|d,-k_{\rm fh}\rangle$ as in Sec. III A. The exciton state $|\text{ex};K\rangle$ can be expanded as $\Sigma_{k_e}\phi(K,k_e)|k_e,k_e-K\rangle$. The envelope function ϕ is approximated by a normalized Lorenzian factor[9]

$$\phi(K,k_e)\equiv\frac{2}{a_0\sqrt{Na_0a}}\left[\left(\frac{1}{a_0}\right)^2+\left(k_e-\frac{\pi}{a}-\frac{W_v}{W_{\rm ex}}K\right)^2\right]^{-1}. \tag{10}$$

W_v and $W_{\rm ex}$ are the bandwidth of the valence and exciton bands, respectively. a_0 is the exciton Bohr radius. In order to get the exciton matrix element, we need to multiply the matrix element for each electron-hole pair by the corresponding envelope function, and sum over all pairs with a given exciton wave number K. Matrix element $M^A_{\rm ex}$ for defect Auger dissociation of exciton through Coulomb scattering is

$$M^A_{\rm ex}(K,k_{\rm fh})\equiv\langle d,-k_{\rm fh}|V_d|\text{ex};K\rangle=\sum_{k_e}\phi(K,k_e)\langle d,-k_{\rm fh}|V_d|k_e,k_e-K\rangle \tag{11}$$

$$=\sum_{k_e=0}^{2\pi/a}\frac{2}{a_0\sqrt{Na_0a}}\left[\left(\frac{1}{a_0}\right)^2+\left(k_e-\frac{\pi}{a}-\frac{W_v}{W_{\rm ex}}K\right)^2\right]^{-1}M_{e\text{-}h}(K,k_h,k_{\rm fh}). \tag{12}$$

$M_{e\text{-}h}$ is given in Eq. (9).

C. Exciton dissociation rate

The rates $W^A(K)$ of defect Auger dissociation for initial exciton wave number K in a chain with N repeat units and one defect can be obtained by summing over all possible final free hole momenta

$$W^A(K)=\frac{2\pi}{\hbar}\sum_{k_{\rm fh}}|M^A_{\rm ex}(K,k_{\rm fh})|^2 \times\delta\{E_{\rm ex}(K)-[\tfrac{1}{2}\varepsilon_g+\Delta\varepsilon-E_v(k_{\rm fh})]\}. \quad (13)$$

The δ function imposes the energy conservation condition. Set the origin of energy at the valence band top, $\Delta\varepsilon$ is the deviation of deep level energy E_d from the mid-gap at $\frac{1}{2}\varepsilon_g$. $E_v(k)$, $E_c(k)$ and $E_{\rm ex}(K)$ are the dispersions for the valence, conduction, and exciton bands, respectively. They are approximated as $E_v(k)=-W_v/2-(W_v/2)\cos(ka)$, $E_c(k)=\varepsilon_g+W_c/2+(W_c/2)\cos(ka)$, and $E_{\rm ex}(K)=\varepsilon_g-\varepsilon_B+W_{\rm ex}/2+(W_{\rm ex}/2)\cos(Ka)$. The corresponding kinetic energy for the bands are defined as $\varepsilon_v(k)\equiv-E_v(k)$, $\varepsilon_c(k)\equiv E_c(k)-\varepsilon_g$, and $\varepsilon_{\rm ex}(K)\equiv E_{\rm ex}(K)-\varepsilon_g+\varepsilon_B$. Their densities of states $\mathcal{G}(\varepsilon)=[\pi|\varepsilon'(k)|]^{-1}$ are $\mathcal{G}_v(\varepsilon)=\{\pi a\sqrt{(W_v/2)^2-[E_v(k)+W_v/2]^2}\}^{-1}$, $\mathcal{G}_c(\varepsilon)=\{\pi a\sqrt{(W_c/2)^2-[E_c(k)-\varepsilon_g-W_c/2]^2}\}^{-1}$, and $\mathcal{G}_{\rm ex}(\varepsilon)=\{\pi a\sqrt{(W_{\rm ex}/2)^2-[E_{\rm ex}(Ka)-\varepsilon_g+\varepsilon_B-W_{\rm ex}/2]^2}\}^{-1}$. $W_{\rm ex}$ is equal to $(1/W_c+1/W_v)^{-1}$ within the effective mass approximation. With these expressions, we can change variable from $k_{\rm fh}$ to $\varepsilon_{\rm fh}$, the final hole kinetic energy, with twofold degeneracy at $+k_{\rm fh}$ and $-k_{\rm fh}$. The rate $W^A(K)$ becomes

$$W^A(K)=\frac{4a_0e^4}{(2\pi)^2\hbar(4\pi\epsilon\epsilon_0)^2N}\frac{1}{\pi a\sqrt{(W_v/2)^2-[\frac{1}{2}\varepsilon_g+\Delta\varepsilon-E_{\rm ex}(K)+W_v/2]^2}} \times\left\{\left(\int_0^{2\pi/a}dk_e\phi'(K,k_e)[\alpha_c m_{D+}(K,k_e)+2\alpha_v m_E(K)]\right)^2 +\left(\int_0^{2\pi/a}dk_e\phi'(K,k_e)[\alpha_c m_{D-}(K,k_e)+2\alpha_v m_E(K)]\right)^2\right\}, \quad (14)$$

where $\phi'(K,k_e)=\{1+[k_e-\pi/a-(W_v/W_{\rm ex})K]^2a_0^2\}^{-1}$, and

$$m_{D\pm}(K,k_e)=\frac{4\pi\epsilon\epsilon_0 a}{2e^2}U-\ln\left\{2\left|\sin\left[\left(\frac{\pi}{a}\pm\frac{1}{a}\cos^{-1}\left(\frac{W_v+2[-E_{\rm ex}(K)+\frac{1}{2}\varepsilon_g+\Delta\varepsilon]}{W_v}\right)+k_e-K\right)\frac{a}{2}\right]\right|\right\}. \quad (15)$$

Note that when the argument of the sin function in Eq. (15) is zero, i.e., $k_{\rm fh}=k_h$ in Eq. (6), $m_{D\pm}$ meets logarithmic singularity, which is integrable in the expression for $W^A(K)$. The rate W^A is, however, not the most convenient quantity to characterize the dissociation efficiency of the defect because it is inversely proportional on the chain size N. In practice, the dissociation rate $1/\tau^A$ is equal to W^A times the number of defect in the chain, which is also proportional

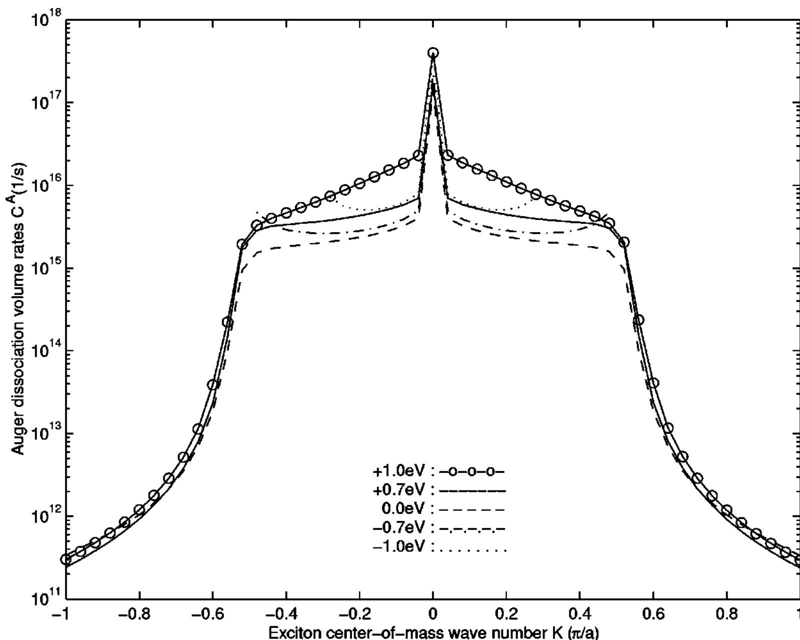

FIG. 2. Volume exciton dissociation rate $c^A(K)$ (see text) for defect Auger process is plotted as a function of the exciton center-of-mass wave number K for various defect level energy $\Delta\varepsilon$ measured from the midgap. The curves for $\Delta\varepsilon=-0.7$ and -1.0 eV stop at $K\approx\pm0.5\pi/a$ and $\pm0.3\pi/a$, beyond which the energy released to the free hole exceeds the valence band width.

to N for a fixed defect density. For convenience, we define a chain size independent quantity $c^A(K)$, the volume dissociation rate, as $W^A(K)N$. The actual dissociation rate $1/\tau^A$ is therefore $c^A(K)$ multiplied by the defect density, defined as the average number of defect per repeat unit. $c^A(K)$ is shown in Fig. 2. The singularity of at $K=0$ is due to the logarithmic divergence of the exchange term $m_E(K)$. Temperature (T) dependence for the thermal averaged rate $c^A(T)$ can obtained by averaging $c^A(K)$ over the exciton wave number K, with the Boltzman weighting factor $\exp(-\beta\hbar^2K^2/2M)$, where M is the sum over electron and hole masses. $c^A(T)$ is shown in Fig. 3. The values of all the parameters used in this paper are listed in Table I. They are designated for PPV.

D. Capture probability for one passage

So far we suppose the center-of-mass wave function of the exciton is a plane wave extended all over the chain. In reality, it is more reasonable to describe the exciton as a wave packet with finite size in the real space. The wave packet diffuses randomly on the polymer chain due to thermal fluctuations. Whether they will be captured (dissociated) by the defect they encounter depends on both the transition rate $1/\tau$, and the interaction time t during which the wave packet covers the defect. t is in turn determined by the incident group velocity $v_g(K)=\partial E_{\text{ex}}/\hbar\partial K$. The capture probability $P^A(t)$ is given by $P^A(t)=1-e^{-t/\tau}$. Note that $P^A(t)=0$ for $t=0$ when the exciton wave packet just starts to hit the defect, and $P^A(t)\simeq 1$ when $t\gg\tau$. The interaction time t is equal to $\xi/|v_g|$, where ξ is the exciton wave packet size alone the chain. On the other hand, the transition rate $1/\tau$ is equal to $c^A(K)a/\xi$, where $c^A(K)$ is the volume dissociation rate, and a/ξ is the effective defect density for the wave packet. t/τ can be then replaced by $c^A(K)a/|v_g(K)|$, in which the unspecified exciton size ξ is cancelled. The passage capture probability is finally given by the simple result

TABLE I. All parameters, suitable for PPV, used in the calculations are listed with references given after the values.

Parameter	Value	Description
a_0	50 Å [8]	Bohr-radius of exciton
a	6.5 Å	Lattice constant
ϵ	2.75 (Ref. 7)	Single chain dielectric constant
W_v	2.3 eV (Ref. 7)	Band width for valance band
W_c	2.0 eV (Ref. 7)	Band width for conduction band
W_{ex}	1.07 eV	Band width for exciton band
ε_g	2.8 eV (Ref. 8)	Energy gap
ε_B	0.34 eV (Ref. 8)	Binding energy of exciton
U	5.1 eV (Ref. 7)	On-site energy
γ	0.25 (Ref. 7)	Correction of U for exchange term
τ_{ph}	40 fs (Ref. 10)	Phonon emission time

$P^A(K)=1-\exp[-c^A(K)a/|v_g(K)|]$. $P^A(K)$ is shown in Fig. 4. It is close to one when the incident velocity v_g is equal to the thermal velocity of 10^5 cm/s at room temperature. The deep levels therefore act as efficient quenching centers, which are crucial for the one-dimensional (1D) diffusion model of PL decay dynamics.[5] $P^A(K)$ drops for higher K because of the decrease of interaction time t for fast exciton passage.

III. IMPACT IONIZATION

The above calculations can be slightly modified to obtain the rate for defect impact ionization, which is the reverse process of defect Auger dissociation. Now the initial state $|d,-k_{\text{fh}}\rangle$ has a free hole with large wave number k_{fh} and a electron in the defect level. There are two possible final states, an exciton $|\text{ex};K\rangle$ with lower threshold and a single electron-hole pair $|k_e,k_{\text{fh}}\rangle$ with higher threshold. They are considered in order below.

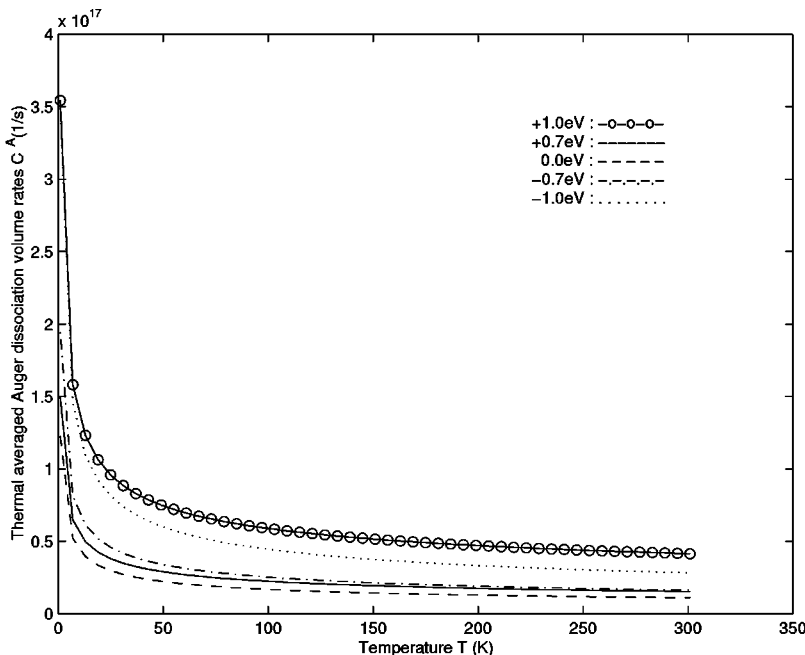

FIG. 3. Thermal averaged volume transition rates c^A of defect Auger exciton dissociation, shown as a function of temperature.

A. Exciton production

The matrix element $M^I_{\rm ex}$ for the creation of an exciton by a hot hole is $\langle {\rm ex},K|V_d|d,-k_{\rm fh}\rangle$. Summing over all possible final states and use the proper density of state $\mathcal{G}_{\rm ex}(\varepsilon_{\rm ex})$ for the exciton, we get the expression for the rate of impact ionization

$$\begin{aligned}W^I_{\rm ex}(k_{\rm fh})&=\frac{2\pi}{\hbar}\sum_K |M^I_{\rm ex}(K,k_{\rm fh})|^2\delta\left\{\left[\frac{1}{2}\varepsilon_g+\Delta\varepsilon-E_v(k_{\rm fh})\right]-E_{\rm ex}(K)\right\}\\&=\frac{4a_0e^4}{(2\pi)^2\hbar(4\pi\epsilon\epsilon_0)^2N}\frac{1}{\pi a\sqrt{(W_{\rm ex}/2)^2-[\frac{1}{2}\varepsilon_g+\Delta\varepsilon-E_v(k_{\rm fh})-\varepsilon_g+\varepsilon_B-W_{\rm ex}/2]^2}}\\&\times\left\{\left(\int_0^{2\pi/a}dk_e\phi'(K,k_e)[\alpha_cM^I_{{\rm ex}D+}(k_e,k_{\rm fh})+2\alpha_vM^I_{{\rm ex}E+}(k_{\rm fh})]\right)^2\right.\\&\left.+\left(\int_0^{2\pi/a}dk_e\phi'(K,k_e)[\alpha_cM^I_{{\rm ex}D-}(k_e,k_{\rm fh})+2\alpha_vM^I_{{\rm ex}E-}(k_{\rm fh})]\right)^2\right\},\end{aligned}$$

where

$$M^I_{{\rm ex}D\pm}(k_e,k_{\rm fh})=\frac{4\pi\epsilon\epsilon_0a}{2e^2}U-\ln\left\{2\left|\sin\left[\left(k_{\rm fh}+k_e-\left[\pm\frac{1}{a}\cos^{-1}\left(\frac{\varepsilon_g+2\Delta\varepsilon-2E_v(k_{\rm fh})-2\varepsilon_g+2\varepsilon_B-W_{\rm ex}}{W_{\rm ex}}\right)\right]\right)\frac{a}{2}\right]\right|\right\},$$

and

$$M^I_{{\rm ex}E\pm}(k_{\rm fh})=\frac{4\pi\epsilon\epsilon_0a}{2e^2}\gamma U-\gamma\ln\left\{2\left|\sin\left[\pm\frac{1}{2}\cos^{-1}\left(\frac{\varepsilon_g+2\Delta\varepsilon-2E_v(k_{\rm fh})-2\varepsilon_g+2\varepsilon_B-W_{\rm ex}}{W_{\rm ex}}\right)\right]\right|\right\}.$$

Similar to Sec. II C, with the above result we get volume ionization rate $c^I_{\rm ex}\equiv W^I_{\rm ex}N$, which is shown in Fig. 5. The corresponding passage probability for impact ionization $P^I_{\rm ex}$ is shown in Fig. 6.

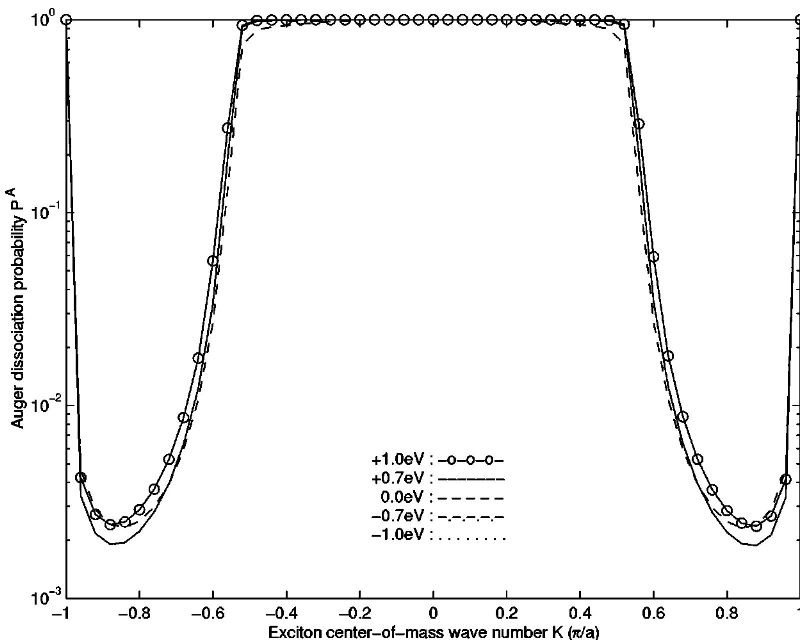

FIG. 4. Dissociation probability $P^A(K)$ of an exciton passing through the defect is plotted as a function of center-of-mass wave number K of exciton. Rise at large K near the zone boundary is due to the smaller group velocity and longer interaction time.

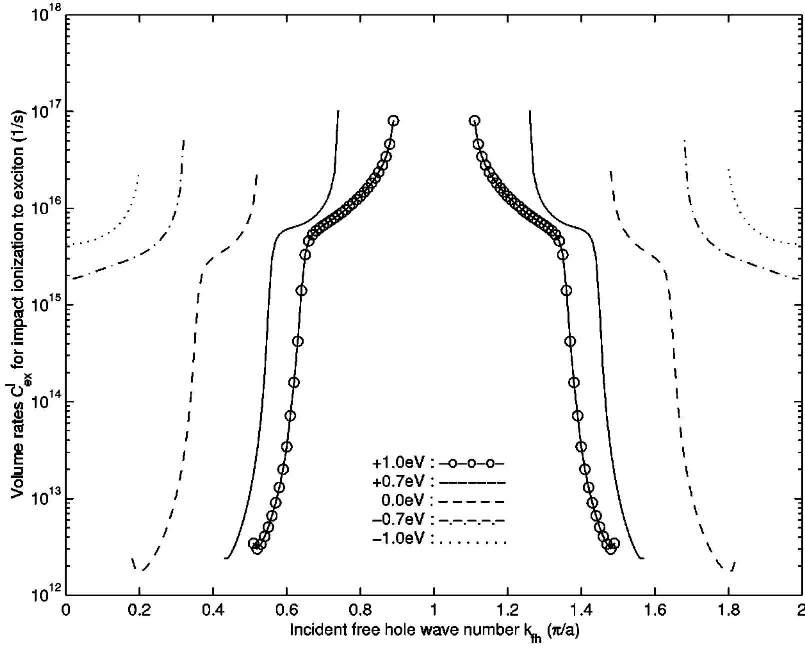

FIG. 5. Volume transition rate c^I_{ex} of defect impact ionization to exciton is shown as a function of incident hot hole momentum $\hbar k_{\text{fh}}$. All curves have threshold momentum required by the energy difference between the defect energy and the exciton energy. The curves of $+1.0$, $+0.7$, and 0.0 eV stop at certain momenta, beyond which no final exciton state satisfies the energy conservation. This is because the exciton band width 1.1 eV is smaller than valence band width 2.3 eV for the incident free hole.

B. Electron-hole pair production

Matrix element $M^I_{e\text{-}h}$ for the creation of a free electron-hole pair is equal to $\langle k_e, k_h | V_d | d, k_{\text{fh}} \rangle$. We sum over k_e and k_h to include all combinations of electron hole pair, and impose the proper energy conservation condition. Integrating over k_h first, we obtain

$$
\begin{aligned}
W^I_{e\text{-}h}(k_{\text{fh}}) &= \frac{2\pi}{\hbar} \sum_{k_e, k_h=0}^{2\pi/a} |M^I_{e-h}(k_e, k_{\text{fh}})|^2 \delta\left\{ E_c(k_e) - E_v(k_h) - \left[\frac{1}{2}\varepsilon_g + \Delta\varepsilon - E_v(k_{\text{fh}}) \right] \right\} \\
&= \frac{e^4}{2\pi^2 \hbar (4\pi\epsilon\epsilon_0 a)^2 N} \left\{ \left[\int_0^{2\pi} dk_e \mathcal{G}'_v(k_e, k_{\text{fh}}) (\alpha_c M^I_{ehD+}(k_e, k_{\text{fh}}) + 2\alpha_v M^I_{ehE+}(k_e, k_{\text{fh}}))^2 \right] \right. \\
&\quad \left. + \left[\int_0^{2\pi} dk_e \mathcal{G}'_v(k_e, k_{\text{fh}}) (\alpha_c M^I_{ehD+}(k_e, k_{\text{fh}}) + 2\alpha_v M^I_{ehE-}(k_e, k_{\text{fh}}))^2 \right] \right\},
\end{aligned}
$$

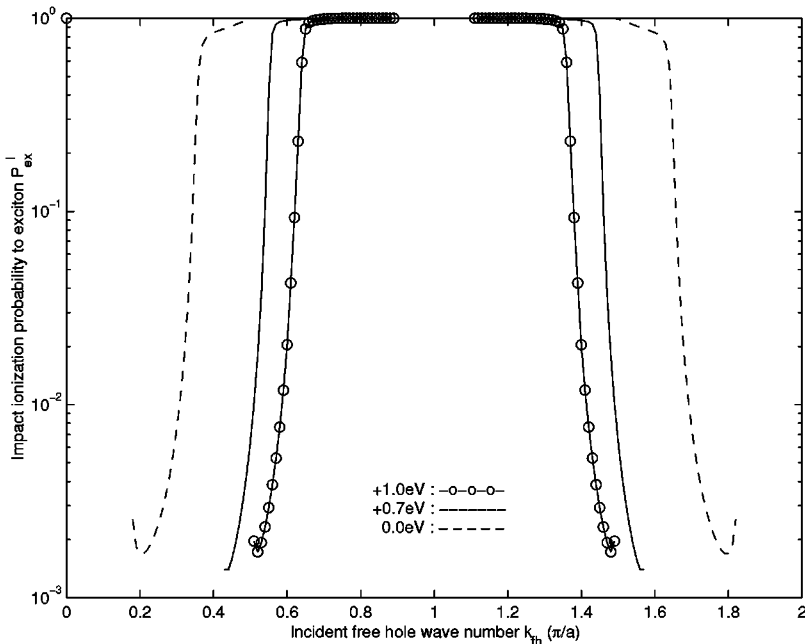

FIG. 6. Probability for the defect impact ionization to exciton state by a hole which passes through the defect with momentum $\hbar k_{\text{fh}}$.

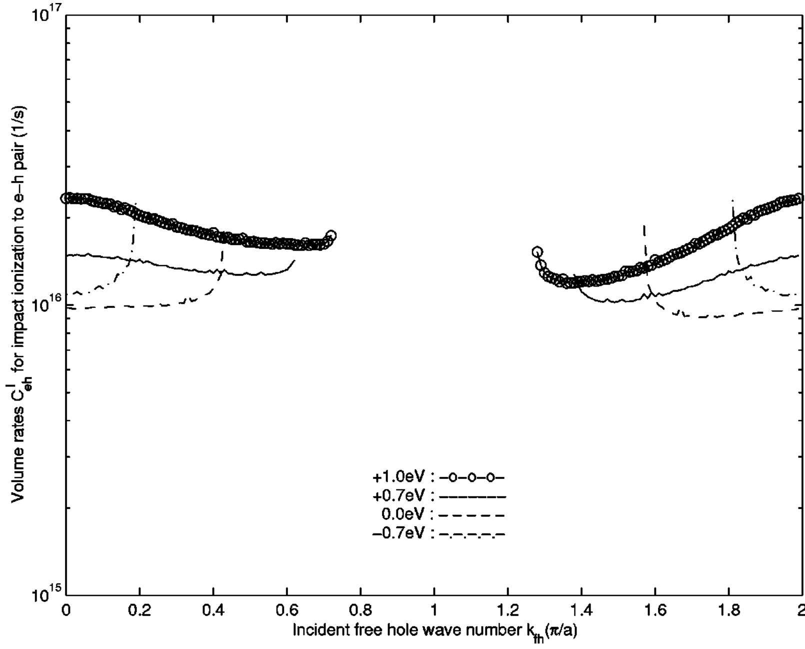

FIG. 7. Volume transition rate $c^I_{e\text{-}h}$ of defect impact ionization to free electron-hole pair by an incident hole with momentum $\hbar k_{\mathrm{fh}}$.

where

$$\mathcal{G}_v'(k_e,k_{\mathrm{fh}})=\frac{1}{\sqrt{(W_h/2)^2-[E_c(k_e)+E_v(k_{\mathrm{fh}})-\frac{1}{2}\varepsilon_g-\Delta\varepsilon+W_v/2]^2}},$$

$$M^I_{ehD\pm}(k_e,k_{\mathrm{fh}})=\frac{4\pi\epsilon\epsilon_0 a}{2e^2}U-\ln\left\{2\left|\sin\left[\left(\frac{\pi}{a}\pm\frac{1}{a}\cos^{-1}\left(\frac{2E_c(k_e)+2E_v(k_{\mathrm{fh}})-2\varepsilon_g-2\Delta\varepsilon+W_v}{W_v}\right)-k_{\mathrm{fh}}\right)\frac{a}{2}\right]\right|\right\}$$

and

$$M^I_{ehE\pm}(k_e,k_{\mathrm{fh}})=\frac{4\pi\epsilon\epsilon_0 a}{2e^2}\gamma U-\gamma\ln\left\{2\left|\sin\left[\left(\frac{\pi}{a}\pm\frac{1}{a}\cos^{-1}\left(\frac{2E_c(k_e)+2E_v(k_{\mathrm{fh}})-2\varepsilon_g-2\Delta\varepsilon+W_v}{W_v}\right)+k_e\right)\frac{a}{2}\right]\right|\right\}.$$

We then perform the k_e integration numerically to get the final result for W^I_{e-h}. Again, we define the volume ionization rate $c^I_{e\text{-}h}(k_{\mathrm{fh}})\equiv W^I_{e\text{-}h}(k_{\mathrm{fh}})N$, which is shown in Fig. 7. The passage probability is not shown, because it is practically one for all wave number above the threshold.

C. Impact ionization coefficient under high electric field

Impact ionization coefficient $\alpha(E)$, defined as the ionization probability per unit drift length of the hot hole, is equal to $W^I(E)/v_d$, where $W^I(E)$ is the avearged impact ionization rate and v_d is the drift velocity for a given electric field E. $W^I(E)$ is obtained from the ensemble average of $W^I(k)$ over the k-distribution function $f_E(k)$ under electric field. Instead of solving the Boltzmann equation for $f_E(k)$ directly, we use the balanced-energy relation to approximate it. The distribution function is assumed to be in the form of a shifted Boltzmann distribution $f_E(k)=\exp[-\varepsilon_v(k-k^*)/(k_BT^*)]$, with two parameters k^* and T^* to be determined self-consistently. k^* is the wave number shift due to the electric field, and is related to the drift velocity v_d by $k^*=m_h v_d/\hbar$. m_h is the hole mass at $k=\pi/a$, the band maximum. The drift velocity v_d is related to the electric field E by $v_d=\mu E$, where the mobility μ is assumed to obey the Drude form $\mu=e\tau_{ph}/m_h$. τ_{ph} is the optical phonon emission lifetime. The effective temperature T^*, which is much larger than the surrounding lattice temperature at high field, is determined by the energy balanced equation $eEv_d=k_BT^*/\tau_{\mathrm{ph}}$.[11] eEv_d is the Joule heating per unit time per unit volume provided by applied field, while $k_BT^*/\tau_{\mathrm{ph}}$ is the thermal power transferred from the electron system to the lattice environment per unit volume. These two quantities must be balanced in steady state. We assume that the all heat comes from optical phonons emitted by the hot holes accelerated by the applied electric field. As W^I discussed above, the impact ionization coefficient α is inversely proportional to the chain size N because there is only one defect on the chain. For convenience, we define the volume ionization co-

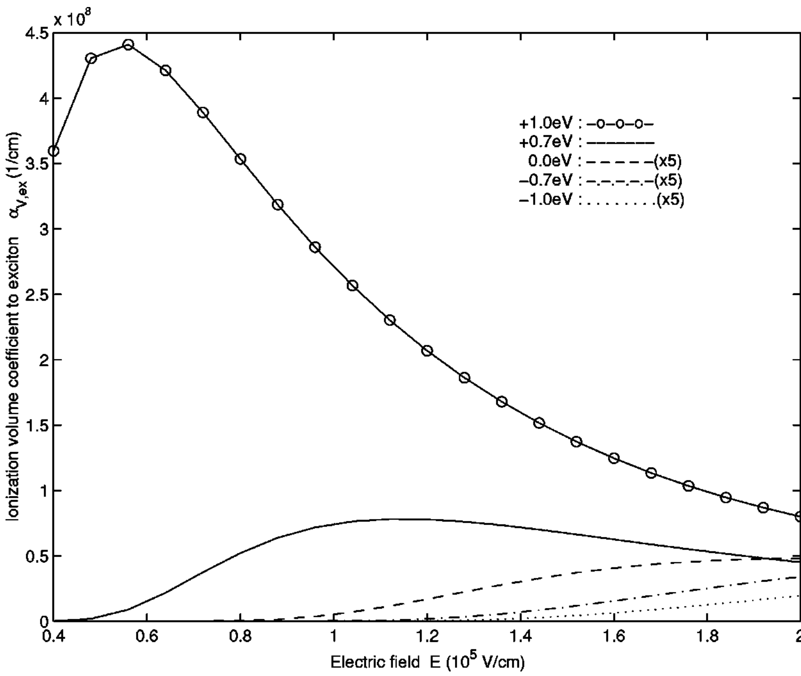

FIG. 8. Impact ionization volume coefficient $\alpha_{V,\mathrm{ex}}$ by a hot hole to exciton under electric field E. The rate grows rapidly as the deep level energy deviation $\Delta\varepsilon$ goes from -1.0 to $+1.0$ eV. In order to distinguish them, we magnify curves for -1.0, -0.7, and 0.0 eV by 5 times.

efficient α_V as αN, such that the actual ionization coefficient on the chain with many defects is equal to α_V times the defect density. $\alpha_{V,\mathrm{ex}}$ and $\alpha_{V,e\text{-}h}$ for the production of excitons and free electron-hole pairs are shown in Figs. 8 and 9, respectively. The free carrier number decreases by one in the former process, and increases by one in the latter. Their difference $\alpha_{V,\mathrm{net}}$, the net carrier production coefficient, is shown in Fig. 10. It is negative when $E \lesssim 2\times 10^5$ V/cm, for which the excitons are the predominant products of the defect impact ionization process, and the net carrier density decreases along the direction of the carrier drift . Light emission is expected from the radiative decay of the excitons.

IV. DISCUSSION

Defect Auger process is well known in inorganic semiconductors,[12] but important only at high carrier densities due to the requirement of the proximity of the second carrier when the first carrier is trapped by the defect. What is special about the similar process in conjugated polymer is that the large binding exciton energy guarantees that each carrier always has an oppositely charged second carrier bound to it and ready to take away relaxation energy, implying an effective high carrier density to facilitate the Auger process. Even though the idea is simple, such a mechanism for exciton dissociation without the need of the third carrier has never

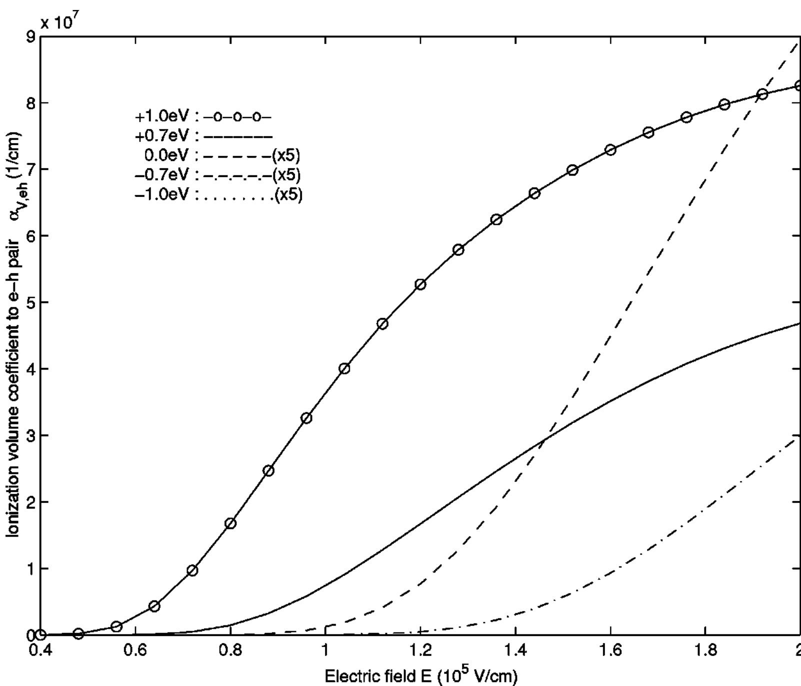

FIG. 9. Impact ionization volume coefficient $\alpha_{V,e\text{-}h}$ to free electron-hole pair by a hot hole under electric field E.

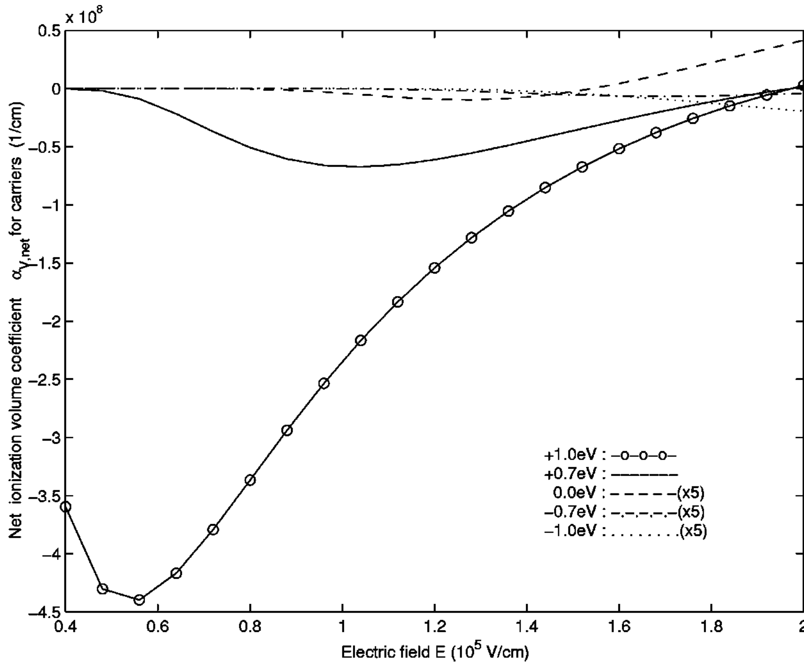

FIG. 10. Volume coefficient $\alpha_{V,\mathrm{net}}$ for the net carrier generation due to impact ionization. $\alpha_{V,\mathrm{net}}$ is equal to $\alpha_{V,e\text{-}h}-\alpha_{V,\mathrm{ex}}$ because the former produces one more carrier and the latter neutralizes the incident hole itself.

been discussed in the literature to our knowledge. Similarly, our prediction of the creation of a neutral bound state instead of more free carriers by impact ionization is also different. These are both good examples that there exist many interesting phenomena in organic semiconductors which are not common in their inorganic counterparts. Novel device operations taking advantage of these phenomena can be envisaged. For instance, exciton production via impact ionization leads to the possibility of light emission under unipolar (single carrier) injection with high field along the chain, i.e., a unipolar LED. When the carrier is accelerated by the field and gains enough kinetic energy to match the difference between the binding energy of the deep level and exciton, the threshold for exciton creation is reached. Our calculation shows that the ionization coefficient for the generation of excitons can be as high as $10^7\ \mathrm{cm}^{-1}$ times the number of defect per repeat unit when the electric field is around $10^5\ \mathrm{V/cm}$ (Fig. 8). When the electric field is further increased the carrier becomes so energetic that the creation of another free carrier out of the defect dominates the creation of excitons. Those carriers are expected to be driven away from each other under such high field and do not recombine to form excitons and emit light anymore. The unipolar light emission is therefore efficient only within a window of electric field. This peculiar behavior can be used as a direct way to verify our prediction experimentally. Such a high field along the chain can not be achieved in the conventional polymer LED with sandwich structure, in which the field is basically perpendicular to the chains. In order to realize this situation, electrodes parallel to the substrate and chain directions must be fabricated. In fact, if the field is high enough, exciton (and unipolar light emission) can be created directly from the ground state via impact ionization even without defects. This will be the subject of further study.

In this work we calculate only the rate by which the electron is captured while the hole is released as the free carrier, mainly because holes have been shown to the the dominant carriers for charge transport due to severe electron trapping in most conjugated polymers.[13,14] The opposite case of electron release and hole trapping can be obtained in almost the same way with similar rate. Only singlet excitons are considered in this work, because the triplet excitons can neither be photoexcited nor emit light. The only difference for the corresponding rates for the triplet excitons is that the contribution from the exchange part of the Coulomb interaction is cancelled.

There are many possible kinds of defects, either structural or chemical, with different binding energy and wave function. For example, the deep level associated with the chain twist varies from the midgap to the bandedge with the twist angle, while the level for oxygen (carbonyl group) is about 0.4 eV below the conduction band in the one-particle picture.[2] The deep level energy will depend on the occupancy if the Coulomb interaction is included. For the case of exciton dissociation by electron trapping, the initial occupation number of the deep level must be either zero or one(at least one vacancy for the electron to fall into). On the other hand, for the case of hole trapping the initial occupation number must be either 1 or 2 (at least one electron to drop into the hole). The impact inonization is just the reverse process of exciton dissociation. The energy of the deep level can be determined, in principle, by the Hartree-Fock self-consistent field. So when the deep level is occupied by one electron, the energy is higher than when the level is empty. Our calculations include all the cases by adjusting the deep level binding energy and the corresponding wave function. Results for deep levels from -1 eV to 1 eV measured from the midgap are shown in the figures. This range covers most of the deep levels revealed by the deep level transient spectroscopy.[15] As for the deep level at the midgap associated with the chain end, the discussion of impact ionization cannot be properly applied. This is because the carrier, and

the resulting exciton, can not travel beyond the chain end. However, the deep level associated with the chain end can still facilitate exciton dissociaton, because the exciton wave function is extended in the conjugated segment and overlaps with the chain end deep level. The center-of-mass wave function of the exciton near the chain end should be more appropriately described by a standing wave (superposition of K and $-K$ states) instead of just a K state. However, according to our calculation the dissociation rate is symmetric under $K\leftrightarrow -K$ inversion, so the result can still apply.

In calculating the impact ionization coefficient we assume that the wave function of the hot carrier interacts with many defects before the ionization, and each carrier experiences the same ionization rate irrespective of its position. The situation is similar to the case of the volume dissociation for exciton quenching. This can be justified because the high kinetic energy of the hot carriers makes them less likely to be localized by the disorder, so they can be described by the extended Bloch states. The excitons at thermal velocity, on the other hand, are much slower and more likely to be localized by disorders.

V. CONCLUSION

We obtain the defect Auger dissociation rate for excitons in conjugated polymers by calculating the matrix element of the Coulomb scattering among three band states and one defect state. Our results show that the defect Auger process is the dominant mechanism for exciton dissociation in EL and photocarrier generation for PC with excitation below the band gap. The capture probability for an exciton passage through the defect is found to be close to one, consistent with the 1D diffusion model for luminescence quenching with non-exponential PL decay. Impact ionization is studied as the reverse process. Exciton creation and the resulting light emission under unipolar carrier injection is predicted for electric field around 10^5 V/cm.

ACKNOWLEDGMENTS

This work is supported by the National Science Council of Taiwan, R.O.C. under Grant No.NSC89-2112-M009-047.

APPENDIX

In this appendix we calculate the matrix element for direct and exchange Coulomb scattering involving one defect state and three band states.

(1) *Direct term* M_D. We start from integration over $\mathbf{r}_2$ in Eq. (3):

$$\int \psi^*_{v,-k_h}(\mathbf{r}_2)\frac{e^2}{4\pi\epsilon\epsilon_0|\mathbf{r}_1-\mathbf{r}_2|}\psi_{v,-k_{\rm fh}}(\mathbf{r}_2)d^3\mathbf{r}_2 = \int e^{-i(k_{\rm fh}-k_h)\mathbf{r}_2}u^*_{v,-k_h}(\mathbf{r}_2)u_{v,-k_{\rm fh}}(\mathbf{r}_2) \times\frac{e^2}{4\pi\epsilon\epsilon_0|\mathbf{r}_1-\mathbf{r}_2|}d^3\mathbf{r}_2, \tag{A1}$$

where $\psi_{\mu,k}(\mathbf{r})=e^{ikr}u_{\mu,k}(\mathbf{r})$ is the Bloch state. Set $\mathbf{r}_2=R+\mathbf{r}$. R is the Bravais lattice vector and $\mathbf{r}$ runs over only one unit cell. Remember that $u_{\mu,k}(\mathbf{r})$ has the period of R. The integration region of $\mathbf{r}_2$ is divided into discrete lattice unit cells. Arranging the summation over R into two groups, one contains $\mathbf{r}_1$ and another one does not, the integral in Eq. (A1) becomes

$$\sum_R \int_{\text{cell at }R} e^{-i(k_{fh}-k_h)(R+\mathbf{r})}u^*_{v,-k_h}(\mathbf{r})u_{v,-k_{fh}}(\mathbf{r}) \times\frac{e^2}{4\pi\epsilon\epsilon_0|\mathbf{r}_1-(R+\mathbf{r})|}d^3\mathbf{r} = \underbrace{\sum_{\mathbf{r}_1\notin R}\int_{\text{cell at }R}\cdots}_{(a)} + \underbrace{\sum_{\mathbf{r}_1\in R}\int_{\text{cell at }R}\cdots}_{(b)} \equiv I_a+I_b.$$

I_a and I_b are approximated separately. In group (a) $\mathbf{r}_2$ is far from $\mathbf{r}_1$, so we take $\mathbf{r}_2\simeq R$, $(\mathbf{r}\simeq 0)$ to get

$$I_a=e^{-i(k_{\rm fh}-k_h)\mathbf{r}_1}\sum_{\mathbf{r}_1\notin R} e^{-i(k_{\rm fh}-k_h)(R-\mathbf{r}_1)} \times\frac{e^2}{4\pi\epsilon\epsilon_0|\mathbf{r}_1-R|}\int_{\text{cell at R}}u^*_{v,-k_h}(\mathbf{r})u_{v,-k_{\rm fh}}(\mathbf{r})d^3\mathbf{r}. \tag{A2}$$

Assuming that the wave number $-k_h$ and $-k_{\rm fh}$ in the last integral can be replaced by π/a, the band edge wave number, we have the approximation $\int_{\text{cell at }R}u^*_{v,-k_h}(\mathbf{r})u_{v,-k_{\rm fh}}(\mathbf{r})d^3\mathbf{r}\simeq 1/N$, where N is the total number of unit cells. This is because that the integration would give unity by normalization if it were integrated over the whole space. But as the integration is over only one repeat unit cell, so it should be equal to $1/N$. I_a is simplified as

$$I_a=e^{-i(k_{\rm fh}-k_h)\mathbf{r}_1}\sum_{\mathbf{r}_1\notin R} e^{-i(k_{\rm fh}-k_h)(R-\mathbf{r}_1)}\frac{e^2}{4\pi\epsilon\epsilon_0|\mathbf{r}_1-R|}\frac{1}{N}.$$

Taking $\mathbf{r}_1$ as the origin and performing the discrete R summation, we get

$$I_a=e^{-i(k_{\rm fh}-k_h)\mathbf{r}_1}\frac{2e^2}{4\pi\epsilon\epsilon_0 a}\frac{1}{N}\left\{-\ln\left[2\left|\sin\frac{(k_{\rm fh}-k_h)a}{2}\right|\right]\right\}.$$

As for I_b, since $\mathbf{r}_2$ is close to $\mathbf{r}_1$ we can set $\mathbf{r}_2=\mathbf{r}_1$ in the exponential term, and take it out of the integration:

$$I_b=e^{-i(k_{\rm fh}-k_h)\mathbf{r}_1}\int_{\text{cell}}u^*_{v,-k_h}(\mathbf{r})u_{v,-k_{\rm fh}}(\mathbf{r})\frac{e^2}{4\pi\epsilon\epsilon_0|\mathbf{r}|}d^3\mathbf{r} = e^{-i(k_{\rm fh}-k_h)\mathbf{r}_1}\frac{U}{N}.$$

U is the on-site Coulomb energy. Adding I_a and I_b together, we get

$$I_a+I_b=\frac{2e^2}{4\pi\epsilon\epsilon_0 a}\frac{1}{N}e^{-i(k_{\mathrm{fh}}-k_h)\mathbf{r}_1}m_D(k_{\mathrm{fh}},k_h),$$

where

$$m_D(k_{\mathrm{fh}},k_h)=\frac{4\pi\epsilon\epsilon_0 a}{2e^2}U-\ln\left[2\left|\sin\frac{(k_{\mathrm{fh}}-k_h)a}{2}\right|\right]. \quad \text{(A3)}$$

Now we integrate over $\mathbf{r}_1$ to get the matrix element M_D.

$$\begin{aligned}M_D(k_e,k_{\mathrm{fh}},k_h)&=\left\{\int_{\mathrm{cell}}\psi_d^*(\mathbf{r}_1)\psi_{c,k_e}(\mathbf{r}_1)e^{-i(k_{\mathrm{fh}}-k_h)\mathbf{r}_1}d^3\mathbf{r}_1\right\}\\&\quad\times\frac{e^2}{4\pi\epsilon\epsilon_0 aN}m_D(k_{\mathrm{fh}},k_h)\\&=\left\{\int_{\mathrm{cell}}u_{c,k_e}(\mathbf{r})\psi_d^*(\mathbf{r})d^3\mathbf{r}\right\}\\&\quad\times e^{-i(k_{\mathrm{fh}}-k_h-k_e+\pi/a)R_d}\frac{e^2}{4\pi\epsilon\epsilon_0 aN}m_D(k_{\mathrm{fh}},k_h)\\&=\frac{\alpha_c}{\sqrt{N}}\frac{e^2}{4\pi\epsilon\epsilon_0 aN}e^{-i(k_{\mathrm{fh}}-k_h-k_e+\pi/a)R_d}m_D(k_{\mathrm{fh}},k_h), \quad \text{(A4)}\end{aligned}$$

where

$$\alpha_c\equiv\int_{\mathrm{all\ space}}u_{c,k_e}(\mathbf{r})\psi_d^*(\mathbf{r})d^3\mathbf{r}=\sqrt{\frac{2}{a\kappa_c}}. \quad \text{(A5)}$$

R_d is the position of defect. α_c is the overlap between u_{c,k_e} and ψ_d. Using the "zero-radius-potential" model[6] to approximate the envelop function of the deep level by the bound state of a 1D δ function potential well, the exponential decay of ψ_d is characterized by the decay coefficient $\kappa_c \equiv\sqrt{2m_c[E_c(k_0)-\frac{1}{2}\varepsilon_g-\Delta\varepsilon]}/\hbar$. $E_c(k_0)-\frac{1}{2}\varepsilon_g-\Delta\varepsilon$ is the defect level binding energy. k_0 is the wave number at the band edge. m_c is the effective mass of the conduction electron at the band minimum. The overlap α_c can be written as $\alpha_c=\sqrt{2/a\kappa_c}=[W_c/(\frac{1}{2}\varepsilon_g-\Delta\varepsilon)]^{1/4}$.

(2) *Exchange term* M_E. Exchanging the subscripts v, $-k_{\mathrm{fh}}$, and c,k_e in M_D [see Eqs. (3) and (4)], and following the similar steps for $m_D(k_{\mathrm{fh}},k_h)$, we obtain

$$\begin{aligned}M_E(k_e,k_h,k_{\mathrm{fh}})=\frac{\alpha_v}{\sqrt{N}}\frac{2e^2}{4\pi\epsilon\epsilon_0 aN}\\\times e^{-i(k_{\mathrm{fh}}-k_h-k_e+\pi/a)R_d}m_E(k_e,k_h),\end{aligned} \quad \text{(A6)}$$

$$m_E(k_e,k_h)=\gamma\left\{\frac{4\pi\epsilon\epsilon_0 a}{2e^2}U-\ln\left[2\left|\sin\frac{(k_e+k_h)a}{2}\right|\right]\right\} \quad \text{(A7)}$$

and

$$\alpha_v\equiv\int_{\mathrm{all\ space}}u_{v,-k_{\mathrm{fh}}}(\mathbf{r})\psi_d^*(\mathbf{r})d^3\mathbf{r}. \quad \text{(A8)}$$

α_v is the overlap between $u_{v,-k_{\mathrm{fh}}}$ and ψ_d, which can be approximated as $\alpha_v=[W_v/(\frac{1}{2}\varepsilon_g+\Delta\varepsilon)]^{1/4}$. The exchange factor γ is defined by

$$\int_{\mathrm{cell\ at\ }R}u_{v,-k_h}^*(\mathbf{r})u_{c,k_e}(\mathbf{r})d^3\mathbf{r}=\frac{\gamma}{N}. \quad \text{(A9)}$$

γ characterizes the overlap between the valence and conduction band states, and is always smaller than 1. The value for γ used in practice is obtained by fitting with the splitting between the singlet and triplet excitons in *ab initio* calculations.[7]

---

*E-mail address: albert.py87g@nctu.edu.tw

†E-mail address: meng@cc.nctu.edu.tw

[1] For review, see R. Friend, R. Gymer, A. Holmes, J. Burroughes, R. Marks, C. Taliani, D. Bradley, D. Dos Santos, J. Brédas, M. Lögdlund, and W. Salaneck, Nature (London) **397**, 121 (1999).

[2] H. Meng and T. Hong, Phys. Rev. B **61**, 9913 (2000).

[3] H. Antoniadis, L. Rothberg, F. Papadimitrakopoulos, M. Yan, M. Galvin, and M. Abkowitz, Phys. Rev. B **50**, 14911 (1994).

[4] D. Moses, J. Wang, G. Yu, and A. Heeger, Phys. Rev. Lett. **80**, 2685 (1998).

[5] M. Yan, L. Rothberg, F. Papadimitrakopoulos, M. Galvin, and T. Miller, Phys. Rev. Lett. **73**, 744 (1994).

[6] V. Abakumov, V. Perel, and I. Yassievich, *Nonradiative Recombination in Semiconductors* (North-Holland, Amsterdam, 1991), p. 227.

[7] The values of the intrachain dielectric constant ϵ, the on-site Coulomb repulsion energy U and the exchange factor γ in Table. I are obtained by fitting our results of single configuration interaction calculation with the first principle calculations by Rohlfing *et al.* [Phys. Rev. Lett. **82**, 1959 (1999)] on the lowest and second lowest singlet and triplet exciton energies.

[8] P. Gomes da Costa and E.M. Conwell, Phys. Rev. B **48**, 1993 (1993).

[9] S. Nakajima, Y. Toyozawa, and R. Abe, *The Physics of Elementary Excitations* (Springer-Verlag, Berlin, 1980).

[10] E.M. Conwell, Phys. Rev. B **57**, R12670 (1998).

[11] K. Seeger, *Semiconductor Physics*, 2nd ed. (Springer-Verlag, Berlin, 1982).

[12] M. Lannoo and J. Bourgoin, *Point Defects in Semiconductors* (Springer-Verlag, Berlin, 1981).

[13] U. Lemmer, R. Mahrt, Y. Wada, A. Greiner, H. Bässler, and E. Göbel, Appl. Phys. Lett. **62**, 2827 (1993).

[14] P. Blom and M. de Jong, IEEE J. Sel. Top. Quantum Electron. **4**, 105 (1998).

[15] H. Gomes, P. Stallinga, H. Rost, A. Holmes, M. Harrison, and R. Friend, Appl. Phys. Lett. **74**, 1144 (1999).